

# Characterization of a Microwave Probe up to Frequencies of 400 GHz

Mark Bieler, Meinhard Spitzer, Günter Hein, and Uwe Siegner

Physikalisch-Technische Bundesanstalt, Bundesallee 100, D-38116 Braunschweig, Germany

**Abstract** — A microwave probe has been characterized up to frequencies of 400 GHz with time-domain sampling techniques. The complex transfer function of the probe as well as the complex reflection and transmission coefficients of transmission line discontinuities have been determined from the time-domain data. This work promotes the time-domain characterization of high-frequency components with coaxial connectors. This task requires the transfer of picosecond electrical pulses between coplanar and coaxial lines, which is often accomplished with microwave probes. Therefore, the detailed propagation characteristics of the probes have to be known for reliable time-domain characterization of coaxial high-frequency devices.

## I. INTRODUCTION

Time-domain sampling techniques allow for the characterization of high-frequency components with a bandwidth that is not accessible with standard electronics such as network analysers [1]. These techniques involve the generation and detection of ultrashort voltage pulses. Voltage pulse generation is usually accomplished with photoconductive (PC) switches, which are embedded in planar structures [2]. Electro-optic (EO) sampling is routinely used to detect the voltage pulses [3]. This technique can only be applied to planar structures in a straightforward way, yet there are many important measurement applications that involve high-frequency components with coaxial connectors. Examples include risetime measurements of broadband oscilloscopes [4] as well as the characterization of picosecond pulse generators and ultrafast photodiodes [5]. Such measurements require the transfer of ultrafast voltage pulses between the coaxial device under test and the planar structures used for pulse generation or detection.

The pulse transfer is often accomplished with microwave probes. Therefore, the propagation characteristics of these probes have to be known for reliable data analysis. Since picosecond voltage pulses involve frequencies well above 100 GHz, the microwave probe characteristics have to be determined in the sub-THz range, even if the cut-off frequency of the probe is lower.

In this paper we characterize a microwave probe that is

attached to a coplanar waveguide (CPW) up to frequencies of 400 GHz. The structure forms a coplanar-coaxial link. We have determined the complex transfer function of the probe as well as the reflection and transmission coefficients of the junction that is formed where the microwave probe is attached to the CPW.

## II. EXPERIMENTAL SET-UP

We have fabricated a CPW onto a 2  $\mu$ m thick low temperature grown (LT) GaAs layer. The LT GaAs was grown at 210 °C and subsequently annealed at 690 °C for 20 minutes. The CPW consists of three 6 mm long, 100 nm thick gold stripes, which have been evaporated onto the semiconductor previously covered with an adhesion layer. The outer stripes are 500  $\mu$ m broad and are separated by 20  $\mu$ m from the 30  $\mu$ m broad center stripe. A 10  $\mu$ m wide gap in the center stripe forms the PC switch (see Fig. 1). To generate the voltage pulses, a bias of 20 V is applied to the CPW and 250 fs laser pulses with an energy of 53 pJ are focused into the PC gap.

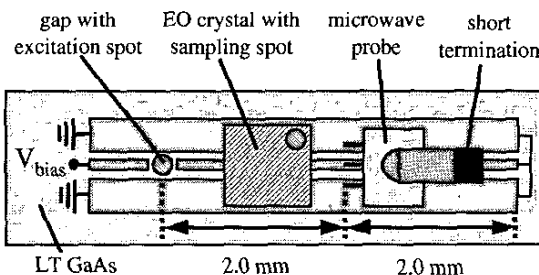


Fig. 1. Experimental set-up. To sample the voltage pulses, the sampling beam is focused on the edge of one of the ground stripes of the CPW.

The voltage pulses on the CPW are detected by EO sampling [3] with a 20  $\mu$ m thick LiTaO<sub>3</sub> crystal placed onto the CPW. The electric field induced refractive index changes in the LiTaO<sub>3</sub> crystal are sampled with 150 fs laser pulses with an energy of 110 pJ. All experiments were performed at room temperature with a 76 MHz titanium:sapphire laser at 840 nm.

The coplanar-coaxial link is realized with a microwave probe (Picoprobe 67A) attached to the CPW 2 mm away

from the CPW end, see Fig. 1. The microwave probe ends in a coaxial connector to which a short termination is attached. Both the microwave probe and the CPW have a characteristic impedance of  $50 \Omega$  at low frequencies.

### III. THEORETICAL MODEL

We model the microwave probe as a spatially uniform element without internal discontinuities. Under this assumption, a complex transfer function of the probe  $H_{\text{probe}} = \exp[-(\delta_{\text{probe}} + i\gamma_{\text{probe}})]$  can be introduced where  $\delta_{\text{probe}}$  and  $\gamma_{\text{probe}}$  are the attenuation and dispersion constants, respectively. In the framework of this transmission line model, reflections at the CPW-probe junction are accounted for by complex reflection and transmission coefficients.

With respect to the measurement of  $H_{\text{probe}}$ , one has to recall the details of the pulse propagation. After generation in the PC gap, picosecond voltage pulses propagate along the CPW towards the CPW-probe junction (forward direction). At the junction they are partially transmitted into the microwave probe. After reflection from the short termination the voltage pulses reach the junction again. Part of them is transmitted onto the CPW where they propagate towards the PC gap (backward direction). The complex transfer function of the round trip  $H_{\text{tot}} = \exp[-(\delta_{\text{tot}} + i\gamma_{\text{tot}})]$  is obtained from EO sampling measurements of the forward propagating ( $E_{\text{in}}$ ) and the backward propagating ( $E_{\text{out}}$ ) voltage pulses at the same position on the CPW.  $H_{\text{tot}}$  can be expressed as follows:

$$\frac{E_{\text{out}}(\omega)}{E_{\text{in}}(\omega)} = H_{\text{tot}} = H_{\text{CPW}} t_1 H_{\text{probe}} H_{\text{short}} H_{\text{probe}} t_2 H_{\text{CPW}} \quad (1)$$

Here  $E_{\text{out}}(\omega)$  and  $E_{\text{in}}(\omega)$  are the Fourier transforms of the time-domain traces  $E_{\text{out}}(t)$  and  $E_{\text{in}}(t)$ . Moreover,  $t_1 = |t_1| \exp[-i\Phi_1]$  and  $t_2 = |t_2| \exp[-i\Phi_2]$  are the complex transmission coefficients of the junction in forward and backward direction, respectively. The transfer function of the CPW is given by  $H_{\text{CPW}} = \exp[-(\alpha_{\text{CPW}} + i\beta_{\text{CPW}})\Delta x]$ , with  $\Delta x$  being the distance from the sampling position to the junction. The transfer function of the short termination is denoted by  $H_{\text{short}}$ . We assume  $H_{\text{short}} = -1$ . Separating amplitude and phase of (1) yields two new equations:

$$\delta_{\text{tot}} = -\ln(|t_1| |t_2|) + 2\delta_{\text{probe}} + \alpha_{\text{CPW}} 2\Delta x \quad (2)$$

$$\gamma_{\text{tot}} = 2\gamma_{\text{probe}} + \beta_{\text{CPW}} 2\Delta x + (\Phi_1 + \Phi_2) + \pi \quad (3)$$

The transmission coefficient  $t_1$  can be calculated from the complex reflection coefficient in forward direction  $r_1$ :

$$t_1 = 1 + r_1 \quad (4)$$

With regard to  $t_2$ , one has to consider that the microwave

probe and the CPW form a T-junction since the probe is not attached to the end of the CPW [6]. Simple analysis of the T-junction shows for arbitrary impedances of the probe and the CPW that the following relation holds:

$$t_2 = -2r_1 \quad (5)$$

The reflection coefficient  $r_1$  as well as  $H_{\text{CPW}}$  and  $H_{\text{tot}}$  can be determined experimentally. Then  $\delta_{\text{probe}}$  and  $\gamma_{\text{probe}}$  can be calculated from (2) - (5).

### IV. EXPERIMENTAL RESULTS

First the propagation parameters of the CPW have been determined. For this purpose the microwave probe was removed from the CPW to avoid reflections from the CPW-probe junction. Two voltage pulses were sampled at different positions spaced by  $\Delta x$ . Taking the Fourier transform of the time traces,  $H_{\text{CPW}}$  can be calculated. Figure 2a shows the mean value of the attenuation constant  $\alpha_{\text{CPW}}$  obtained by averaging over four independent measurements. Figure 2b shows the effective dielectric constant  $\epsilon_{\text{eff}} = (\beta_{\text{CPW}} c/\omega)^2$  calculated from the mean value of  $\beta_{\text{CPW}}$  ( $c$  speed of light in vacuum).

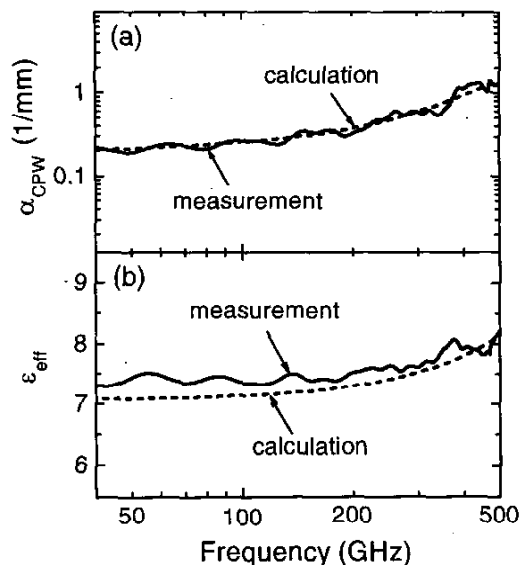


Fig. 2. Attenuation constant  $\alpha_{\text{CPW}}$  and effective dielectric constant  $\epsilon_{\text{eff}}$  of the CPW. Solid lines: experimental data (mean values). Dashed lines: calculations following [7], [8] and [9].

The experimental data are compared to theoretical predictions. The attenuation constant of the CPW has been calculated accounting for radiation losses [7] and conductor losses [8]. Dielectric losses are negligible [7].

The effective dielectric constant has been calculated with the model derived by Hasnain *et al.* [9]. The calculations were performed with an experimentally determined conductivity  $\sigma = 3 \times 10^7 \text{ (}\Omega\text{m)}^{-1}$  of the metal contacts. The experimental data for  $\alpha_{\text{CPW}}$  and  $\epsilon_{\text{eff}}$  agree very well with the calculations, testifying to the reliability of the experimental procedure.

To determine the reflection coefficient of the CPW-probe junction, the microwave probe was attached to the CPW. The time-domain signal sampled midway between the excitation gap and the junction consists of the incident voltage pulse and the reflection from the junction [6]. When the voltage pulse is sampled at the same position without an attached microwave probe, only the incident signal is recorded. Subtraction separates the reflected signal from the incident one. From the Fourier transforms of the reflected and incident pulses the reflection coefficient  $r_1$  is calculated. The propagation of the pulses on the CPW is considered in our analysis. Mean values of the amplitude and phase of  $r_1$  were obtained from four independent measurements. Using (4) and (5) with these mean values, the complex transmission coefficients  $t_1$  and  $t_2$  have been determined. The amplitudes and phases of  $r_1$  (mean value),  $t_1$ , and  $t_2$  are plotted in Fig. 3.

Figure 3a shows that the amplitudes of  $t_1$  and  $t_2$  are rather similar at low frequencies, but differ from each other more strongly at higher frequencies. We like to note that  $t_1$  and  $t_2$  are equal if and only if the impedances of the CPW and the probe are equal. This statement does not contradict the reciprocity theorem for scattering matrices since the scattering matrix formalism considers power waves while the transmission coefficients connect voltages. The amplitude of  $r_1$  is almost constant at lower frequencies and shows larger variations as the frequency is increased. All phases are close to 0 or  $\pi$ .

If the reflection coefficient  $r_1$  is calculated for the nominal low-frequency impedances of the CPW and the microwave probe of  $50 \Omega$ ,  $r_1 = -1/3$  is obtained accounting for the T-junction. Equations (4) and (5) then yield  $t_1 = t_2 = 2/3$ . The experimental curves are in line with the results calculated for  $50 \Omega$  impedances up to frequencies of 250 GHz. The deviations at higher frequencies indicate that the impedances deviate from  $50 \Omega$ .

To determine the transfer function  $H_{\text{tot}}$  of the round trip, i.e.,  $\delta_{\text{tot}}$  and  $\gamma_{\text{tot}}$ , we have made use of (1). For the measurement of  $E_{\text{in}}$  the microwave probe was lifted off the CPW to avoid reflections. Mean values of  $\delta_{\text{tot}}$  and  $\gamma_{\text{tot}}$  have been calculated from the results of four independent measurements. These mean values together with the data in Figs. 2 and 3 have been used to calculate the

attenuation constant  $\delta_{\text{probe}}$  and the dispersion constant  $\gamma_{\text{probe}}$  of the microwave probe using (2) and (3). The dispersion constant  $\gamma_{\text{probe}}$  mainly reflects the propagation time over the microwave probe of 207 ps (data not shown). In fact, the group delay  $d\gamma_{\text{probe}}/d\omega$  is almost constant up to 200 GHz.

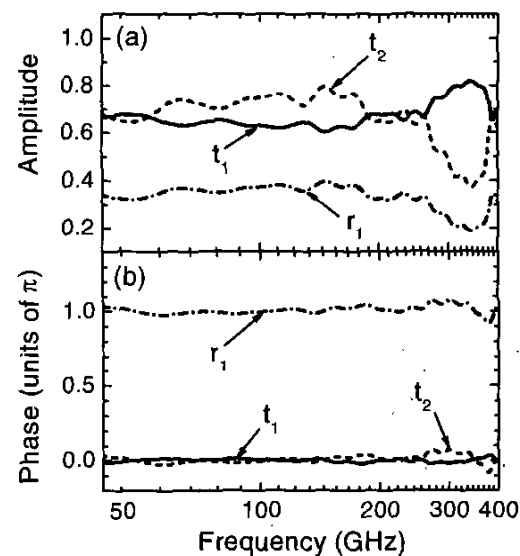


Fig. 3. Amplitude (a) and phase (b) of the complex reflection coefficient  $r_1$  (dashed-dotted) and the complex transmission coefficients  $t_1$  (solid) and  $t_2$  (dashed).

We will now discuss the attenuation of the microwave probe and compare it to the attenuation terms resulting from the CPW and the CPW-probe junction. To simplify the comparison, we distinguish between the forward direction (involving the transmission coefficient  $t_1$ ) in Fig. 4a and the backward direction (involving  $t_2$ ) in Fig. 4b. The forward-direction data are relevant for oscilloscope risetime measurements while the backward-direction data can be used when a pulse generator or a photodetector with a coaxial output connector is characterized. To quantify the attenuation, we have plotted the loss in dB, i.e.,  $20 \log[\exp(-\delta_{\text{probe}})]$ ,  $20 \log[t_1]$ ,  $20 \log[t_2]$ , and  $20 \log[\exp(-\alpha_{\text{CPW}} \Delta x)]$  for  $\Delta x = 0.5 \text{ mm}$ , which is a typical propagation distance on the CPW. The sum of the loss terms is also shown.

The results show that the loss of the microwave probe is smaller than 1.3 dB for frequencies below 60 GHz, in agreement with the specifications of the manufacturer. The probe loss increases to 3 dB if the frequency is raised to 150 GHz. In this frequency range, the overall frequency

dependence of the probe loss is still weak. Above 150 GHz the loss strongly increases, reaching 10 dB at 210 GHz. Above 210 GHz resonances are observed in the probe loss. We attribute these resonances to the excitation of higher modes. The loss of the CPW is smaller than 5 dB up to 400 GHz. Thus, the CPW is not the limiting factor for the transfer of ultrashort voltage pulses, as expected. The losses corresponding to  $t_1$  vary between 1.8 dB and 4.4 dB in the range from 40 GHz to 400 GHz without a pronounced frequency dependence. The transmission coefficient  $t_2$  gives rise to losses between 2 dB and 8.6 dB where losses of more than 4 dB occur only for frequencies above 260 GHz. The junction loss dominates below 160 GHz (120 GHz) in forward (backward) direction. If the microwave probe can be attached at the end of the CPW to avoid the T-junction, these contributions can be reduced. The total loss for both directions is smaller than 10 dB and only weakly frequency dependent up to 150 GHz. At higher frequencies the loss of the microwave probe dominates the total loss. Further calculations demonstrate that, despite its frequency dependence, the total loss in forward direction allows the generation of a 4 ps pulse at the coaxial connector of the microwave probe if a 2 ps pulse is launched on the CPW.

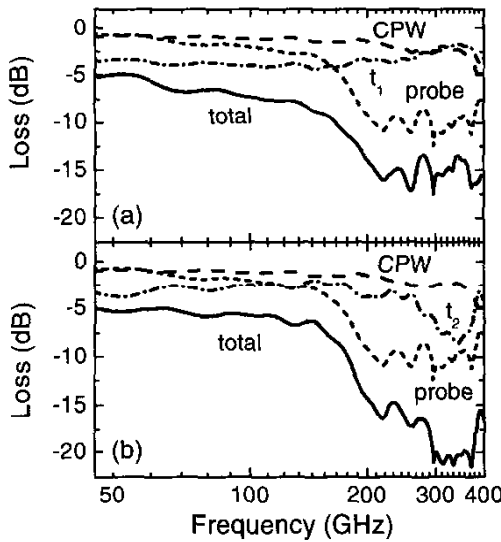


Fig. 4. (a) Forward direction (from the CPW to the probe). Probe loss (short-dashed), junction loss (dashed-dotted), CPW loss (long-dashed), and total loss (solid). (b) Same for backward direction. The probe loss and the CPW loss are the same in (a) and (b).

## V. CONCLUSION

We have determined the attenuation and dispersion constants of a microwave probe as well as the transmission coefficients of the junction formed by the probe and a coplanar waveguide up to 400 GHz. These data can be used to predict the output pulse of the coplanar-coaxial link realized by our set-up for arbitrary input pulses in this frequency range.

## ACKNOWLEDGEMENT

The authors like to thank T. Schrader, U. Arz, R. Doerner and W. Heinrich for useful discussions. The LT GaAs was grown by P. Specht and E. R. Weber, University of California at Berkeley, supported by the AFOSR grant F49620-01-1-0151.

## REFERENCES

- [1] M. Y. Frankel, J. F. Whitaker, G. A. Mourou, and J. A. Valdmanis, "Ultrahigh-bandwidth vector network analyzer based on external electro-optic sampling," *Solid-State Electronics*, vol. 35, pp. 325-332, 1992.
- [2] D. H. Auston, "Impulse Response of Photoconductors in Transmission Lines," *IEEE J. Quantum Electron.*, vol. 19, pp. 639-648, 1983.
- [3] J. A. Valdmanis and G. A. Mourou, "Subpicosecond electrooptic sampling: principles and applications," *IEEE J. Quantum Electron.*, vol. 22, pp. 69-78, 1986.
- [4] A. J. A. Smith, A. G. Roddie, and D. Henderson, "Electrooptic sampling of low temperature GaAs pulse generators for oscilloscope calibration," *Optical and Quantum Electronics*, vol. 28, pp. 933-943, 1996.
- [5] P. D. Hale, T. S. Clement, D. F. Williams, E. Balta, and N. D. Taneja, "Measuring the Frequency Response of Gigabit Chip Photodiodes," *J. Lightwave Tech.*, vol. 19, pp. 1333-1339, 2001.
- [6] M. Bieler, M. Spitzer, G. Hein, and U. Siegner, "Time-domain characterisation of non-coplanar high-frequency components up to 300 GHz," *Electron. Letters*, vol. 38, pp. 1038-1039, 2002.
- [7] M. Y. Frankel, S. Gupta, J. A. Valdmanis, and G. A. Mourou, "Terahertz attenuation and dispersion characteristics of coplanar transmission lines," *IEEE Trans. Microwave Theory Tech.*, vol. 39, pp. 910-916, 1991.
- [8] C.-L. Liao, Y.-M. Tu, J.-Y. Ke, and C. H. Chen, "Transient propagation in lossy coplanar waveguides," *IEEE Trans. Microwave Theory Tech.*, vol. 44, pp. 2605-2611, 1996.
- [9] G. Hasnain, A. Dienes, and J. R. Whinnery, "Dispersion of picosecond pulses in coplanar transmission lines," *IEEE Trans. Microwave Theory Tech.*, vol. 34, pp. 738-741, 1986.